IV Journeys in Multiphase Flows (JEM2017)
March 27-31, 2017 - São Paulo, Brazil

PaperID: JEM-2017-0025

EXPERIMENTAL EVALUATION OF DYNAMIC STRUCTURAL PARAMETERS AND DESIGN GUIDELINES FOR TUBES UNDER TWO-PHASE CROSSFLOW INDUCED VIBRATION

Ricardo Álvarez-Briceño [1]
Fabio Toshio Kanizawa [2]
Gherhardt Ribatski[1,3]
Leopoldo P. R. de Oliveira[1]
[1] Mechanical Engineering Department, São Carlos School of Engineering, University of São Paulo, Av. Trabalhador São Carlense, 400, Parque Arnold Schmidt, São Carlos, São Paulo, CEP 13566-590, Brazil
[2] Federal Fluminense University
[3] Heat Transfer Research Group
r.alvarezbriceno@gmail.com
fabio.kanizawa@mec.uff.br
ribatski@sc.usp.br
leopro@sc.usp.br

Abstract. *The present paper addresses an experimental investigation of flow-induced vibration (FIV) during two-phase air-water flow across a normal triangular tube bundle, counting with tubes of 19 mm O.D. and transverse pitch per diameter ratio of 1.26. The experimental approach features a tube mounted in cantilever, which is instrumented with two accelerometers perpendicularly mounted in the free tip. Based on measured acceleration power spectral densities, a study on dynamic parameters, such as hydrodynamic mass and damping ratio, is performed. Moreover, its variation with homogeneous void fractions ranging from 30% to 95% is analyzed and compared with results found in open literature. Furthermore, the current models used to predict the tube vibration upper-bound during FIV induced by turbulence-induced mechanism are reviewed and implemented for the conditions of the experimental database from the present experimental campaign and gathered in the open literature. The dynamic parameters estimated with predictive methods showed good agreement with the experimental database, as well as the design guidelines for FIV induced by turbulence showed to be a reasonable design tool.*

Keywords: *cantilever-beam, flow-induced vibration, two-phase flow, void fraction, dynamic parameter*

1. INTRODUCTION

Flow-Induced Vibration (FIV) is the most critical dynamic issue in the design of shell-and-tube heat exchangers. This fluid-structure phenomenon may generate high amplitude vibration of tubes or structural parts, which leads to fretting wear between the tubes and supports, noise or even fatigue failure of internal components. The study of this phenomenon is more challenging if considered that two-phase crossflow exists in more than half of shell-and-tube heat exchangers used in industry (Green and Hetsroni, 1995; Noghrehkar *et al.*, 1999). In fact, void fraction and flow patterns do affect the dynamic parameters of the vibrating tube *e.g.* hydrodynamic mass and damping ratio (Carlucci and Brown, 1983; Pettigrew *et al.*, 1989; Lian *et al.*, 1997; Pettigrew and Taylor, 2004). Furthermore, tests have shown that vibration levels induced by two-phase flow can be more severe than in single-phase flow (Taylor *et al.*, 1989), and the mechanism promoting this vibration may be distinct from flow turbulence (Axisa *et al.*, 1990). However, in spite of the importance of devices subjected to two-phase flow, FIV under these conditions have not been entirely understood. In this manner, more studies intended to clarify the behavior of the dynamic parameters and the insights of the mechanism of turbulence-induced vibration in two-phase flow are needed.

In order to increase the current data base and study those missing details on hydrodynamic mass, two-phase damping ratio under two-phase flow, a test bench was designed and constructed. Parameters such as resonance frequencies, and damping ratios are obtained from power spectral densities measured by an instrumented tube, which is mounted in cantilever and surrounded by tubes fixed at both ends mimicking a configuration of a heat exchanger tube bundle. Results on dynamic parameters are compared with results and models in open literature. Furthermore, turbulence - induced vibration design guidelines are checked for the present result. The experimental apparatus description, experimental results and conclusions are detailed in the foregoing sections.

2. DYNAMIC PARAMETERS

The dynamic response of a vibrating tube in a heat exchanger depends on its inertia, stiffness and energy dissipaters (damping), which are referred to as the dynamic parameters. The system's damping and inertia measured during two-phase flow are quite different from that measured in air or water single-phase flows, while stiffness is assumed to be constant as flow velocity is considerably away from fluidelastic instability threshold. Furthermore, damping and hydrodynamic mass are known to depend on fluid properties as well as on the component geometry and adjacent boundaries, whether rigid or elastic (Khushnood *et al.*, 2012). In the subsections below, hydrodynamic mass and damping ratio are defined according to the literature.

2.1 Hydrodynamic mass

Hydrodynamic mass, also referred to as added mass or virtual mass, is defined as the equivalent mass of external fluid vibrating with the structure (Pettigrew and Taylor, 1994), in this case a tube. It increases the apparent inertia of the vibrating body, but the stiffness remains the same, hence modifying the tube dynamic behavior. Carlucci and Brown (1983) studied hydrodynamic mass of a single cylinder in axial two-phase flow simulated by air-water mixtures. They deduced experimentally the hydrodynamic mass per unit length of the cylinders, m_h, in terms of the resonance frequency of the cylinder in two-phase mixture, f, as follows:

$$m_h = m_t \left[\left(\frac{f_g}{f} \right)^2 - 1 \right], \tag{1}$$

where m_t is the mass of the tube alone per unit length and f_g is the resonance frequency of the tube in air. In this manner, one can understand the variation of m_h in terms of the variation of f depending on the flow characteristics.

On the other hand, the hydrodynamic mass of a tube vibrating in a bundle can also be predicted by the theoretical model of Rogers *et al.* (1984) for liquid flow:

$$m_h = \left(\frac{\rho \pi d^2}{4} \right) \left[\frac{(D_e/d)^2 + 1}{(D_e/d)^2 - 1} \right], \tag{2}$$

where d is the tube diameter. The term (D_e/d) represents the effect of confinement for a tube inside a triangular tube bundle, which is formulated by:

$$\frac{D_e}{d} = \left(0.96 + 0.5 \frac{P}{d} \right) \frac{P}{d}, \tag{3}$$

in which P is the transverse pitch of the tube bundle, and the density, ρ, must be assumed equal to the average density of the mixture $\bar{\rho}$, at superficial void fraction α, also referred as area averaged void fraction, rendering:

$$\bar{\rho} = \rho_l (1 - \alpha) + \rho_g \alpha \tag{4}$$

Furthermore, for the present analysis, as generally adopted in open literature, void fraction is estimated with the homogeneous model. Thus, it is admitted equal superficial velocity of both phases, which is also equal to the average velocity of the mixture.

2.2 Damping ratio

Damping is the parameter of the system that represents the dissipative process. Carlucci (1980) suggested that, for examining damping in a tube bundle, the total damping can be modeled as a sum of three components: structural damping, ζ_S, viscous damping based on homogeneous two-phase parameters, ζ_V, and the two-phase damping component, ζ_{TP}. The structural component is related to damping by means of tube material and mounting configuration. The viscous component of damping in two-phase mixtures is taken to be analogous to viscous damping in single-phase fluids, as introduced by Pettigrew *et al.* (1986):

$$\zeta_V = \frac{100\pi}{\sqrt{8}} \left(\frac{\bar{\rho} d^2}{m} \right) \left(\frac{2\nu_{TP}}{\pi f d^2} \right)^{0.5} \left\{ \frac{\left[1 + (d/D_e)^3 \right]}{\left[1 - (d/D_e)^2 \right]^2} \right\}, \tag{5}$$

where ζ_V is the viscous damping ratio in percent, m is the tube mass per unit length including the hydrodynamic mass and ν_{TP} is the kinematic two-phase viscosity evaluated according the McAdams model (Collier and Thome, 1994).

On the other hand, the two-phase damping ratio is perhaps the most complex parameter to be evaluated in this analysis. Theoretical models formulated by Blevins (2001) and Païdoussis *et al.* (2011) argue that damping ratio depends on mass

velocity since they state that the effective damping of a cylinder in crossflow is a function of flow velocity and fluid density. Despite these analytical approaches for a single cylinder in crossflow, experimental studies on damping of tubes in tube bundles (Carlucci, 1980; Carlucci and Brown, 1983; Pettigrew *et al.*, 1989) show that the dependence of two-phase damping ratio on flow velocity is marginal. Furthermore, results reported in open literature (Carlucci and Brown, 1983; Pettigrew *et al.*, 1989; Lian *et al.*, 1997; Pettigrew *et al.*, 2001) show that two-phase damping ratio does vary significantly with void fraction. In fact, these references mention a peaking behavior of two-phase damping with homogeneous void fraction, with maximum damping at intermediate void fractions. The peaking behavior was only better understood after the study performed in Lian *et al.* (1997). They found that the root mean square (RMS) amplitude of local void fraction fluctuations increases up to a void fraction of 40% during bubbly flow pattern, reaches a peak at about 50% and then decreases gradually with additional void fraction increment in the intermittent and annular-dispersed droplet flow patterns. The relationship between local void fraction fluctuations and damping ratio makes sense, since there are large temporal fluctuations in the fluid momentum whenever gas and liquid slugs alternately impinge on the vibrating tube in intermittent flow. This means that there is a fluid force associated with these rapid changes in fluid momentum and, if this force causes displacement of the tube, there will be energy transfer between the tube and the fluid (Lian *et al.*, 1997).

Pettigrew and Taylor (2004) presented a semi-empirical formulation for two-phase damping ratio based on the experimental database available until that year. A well structured review is presented by Pettigrew and Taylor (2004), from which it can be summarized that two-phase damping is strongly dependent on void fraction and flow patterns, which in turn are somehow linked by mass velocity, even though it was found that mass velocity *per se* is not an important parameter in damping analysis. Furthermore, two-phase damping is directly related to confinement and to the mass ratio ($R = m/\rho_l d^2$), whose influence can be formulated and used to normalize two-phase damping ratio data. Moreover, ζ_{TP} is weakly related to the tube resonance frequency and tube bundle configuration. Following these arguments, Pettigrew and Taylor (2004) approximated two-phase damping as:

$$\zeta_{TP} = A \cdot \left(\frac{\rho_l d^2}{m}\right) \cdot \varphi(\alpha) \cdot C(D_e/d), \tag{6}$$

where A is an overall coefficient determined experimentally, which according to the authors is equal to 0.04. The effect of confinement is best formulated by the confinement function $C(D_e/d)$:

$$C(D_e/d) = \frac{\left[1 + (d/D_e)^3\right]}{\left[1 - (d/D_e)^2\right]^2} \tag{7}$$

The function $(\rho_l d^2/m)$ is the inverse of the mass ratio, calculated for the liquid density ρ_l, and $\varphi(\alpha)$ is a void fraction function, which was approximated aiming to present a similar shape to the collapsed available (at that time) experimental data:

$$\varphi(\alpha) = \begin{cases} \frac{\alpha}{40} & \text{for } \alpha < 40\% \\ 1 & \text{for } 40\% < \alpha < 70\% \\ 1 - \frac{\alpha - 70}{30} & \text{for } 70\% < \alpha \end{cases} \tag{8}$$

where the void fraction α is given as percentage. Lately, Sim (2007) proposed a semi-analytical model for estimating the total damping ratio in the transverse direction. However, this model is not reviewed in the present study since its implementation requires an additional discussion on void fraction models, which is beyond the scope of the present paper.

3. TURBULENCE-INDUCED VIBRATION

The vibration response below the threshold velocity for fluidelastic instability is attributed to random turbulence excitation (Pettigrew *et al.*, 2001). In this context, the turbulence that is referred to is the turbulence level of the incoming flow in the tube bundle, as well as the turbulence generated by the passage across the upstream rows. Usually, this vibration mechanism will not lead to catastrophic failure; however there is a practical need for the designer of heat exchangers to be aware of the magnitude of vibration levels caused by two-phase flow so that fretting-wear and fatigue can be avoided throughout the required heat exchanger lifetime. Various methods have been developed to analyze, collapse and normalize the available experimental data sets so that models can be proposed in order to define an upper bound envelope of two-phase flow-induced forces under certain operational conditions. The methods developed by Taylor *et al.* (1989), Papp and Chen (1994) and de Langre and Villard (1998) are described below.

3.1 Model proposed by Taylor *et al.* (1989)

The model developed by Taylor *et al.* (1989) normalizes the excitation PSD, $S_F(f)$, by using the mass velocity and the tube diameter. This data reduction is based on the assumption that the RMS amplitude is directly proportional to the

reference gap mass velocity and to the tube diameter, which for the present test section was checked in Álvarez-Briceño *et al.* (2016). Thus, the normalized power spectral density ($NPSD$) is defined by Taylor *et al.* (1989) as follows:

$$NPSD = \frac{S_F(f)}{(Gd)^2} \tag{9}$$

Based on the data reduced according to Eq.9, Taylor *et al.* (1989) defined a design guideline for $NPSD$ as a function of void fraction, α:

$$NPSD = 10^{(3\alpha-5)}, \tag{10}$$

which actually is an upper bound envelope based on experimental data.

3.2 Model proposed by Papp and Chen (1994)

Papp and Chen (1994) proposed a correlation to estimate the RMS vibration displacement, $\bar{y^2}$, based on the hypothesis that the momentum transfer from the fluid to structure by means of mechanical vibration is mainly related to the mechanical energy of the flow, which variation corresponds to pressure drop. Thus, the RMS vibration displacement is given by:

$$\left(\bar{y^2}\right)^{0.5} = C_I \cdot \phi_{L0}^2 \cdot Eu_{L0} \left(\frac{C_1}{16\pi^3 f^3 m^2 \zeta}\right)^{0.5} \frac{G^2}{2\rho_l} d \tag{11}$$

where $C_1 = 0.613$ for cantilevered tubes at maximum displacement point, ϕ_{L0} is the two-phase friction multiplier calculated according to the correlation of Grant and Chisholm (1979), Eu_{L0} is the Euler number evaluated according to Zukauskas and Ulinskas (1983) and C_I is the coefficient of interaction. This model tries to characterize the relationship between the tube response, flow parameters and structural parameters through C_I. According to Papp and Chen (1994), the highlight of this model is that it takes into account all the parameters of a coupled fluid-tube system; i.e.: (i) the two-phase multiplier is a function of two-phase flow parameters (void fraction, mass velocity, pressure); (ii) the Euler number (Eu_{L0}) depends on tube bundle geometry; and (iii) the dynamic characteristics of the tube such as: mass, damping, resonance frequency and boundary conditions of mounting. Furthermore, Papp and Chen (1994), based on experimental results obtained in Taylor *et al.* (1989) propose two constant values of C_I for two void fraction intervals, for $\alpha \leq 50\%$ and for $\alpha > 50\%$. These values are tabulated in Papp and Chen (1994). Additionally, they are plotted as reference lines in Fig. 9 in order to compare experimental results obtained in the present work.

3.3 Model proposed by de Langre and Villard (1998)

De Langre and Villard (1998), based on previous work of Axisa *et al.* (1990), found a scaling procedure capable of reducing the experimental force spectrum data and collapsing the results obtained for two-phase flow. In this manner, de Langre and Villard (1998) proposed an upper-bound for the dimensionless reference equivalent force spectrum, $\left[\bar{\Phi_E^0}\right]_U$, given by:

$$\left[\bar{\Phi_E^0}\right]_U = 10 \cdot f_R^{-0.5} \quad \text{for} \quad 10^{-3} \leq f_R \leq 0.06 \tag{12}$$

$$\left[\bar{\Phi_E^0}\right]_U = 2 \cdot 10^{-3} f_R^{-3.5} \quad \text{for} \quad 0.06 \leq f_R \leq 1 \tag{13}$$

Moreover, the RMS displacement contributed by the mode n can be formulated in terms of $\left[\bar{\Phi_E^0}\right]_U$ as:

$$\left[y_n^2(x)\right]^{0.5} = \left[\frac{\varphi_n^2(x) L^2 a_n}{64\pi^3 f_n^3 M_n^2 \zeta_n} (\rho_l g D_w d)^2 \frac{D_w}{U_p} \left(\frac{L_0}{L}\right) \left(\frac{D}{D_0}\right) \left[\bar{\Phi_E^0}\right]_U\right]^{0.5} \tag{14}$$

where L is the tube length, M_n is the tube total mass (including hydrodynamic mass), ζ_n is the total damping ratio and f_n is the resonance frequency. The modal shape, $\varphi_n(x)$, and the modal correlation factor, a_n, are equal to 2 and 0.5, respectively, as tabulated for cantilevered tubes in Pettigrew and Taylor (2003). The reference lengths are $L_0 = 1$m and $D_0 = 0.02$m, and g represents the gravitational acceleration.

4. THE TEST BENCH

This section describes the test bench used during the experimental campaign including its general configuration, measurement system, as well as the flow patterns observed during the present study, which were firstly described by Kanizawa

and Ribatski (2016a). Furthermore, the models proposed by Kanizawa and Ribatski (2015, 2016c) to estimate superficial void fraction and pressure drop across a tube bundle are introduced. These models, which are based on experimental data measured in the present experimental facility, will be adopted in a subsequent analysis of the design guideline proposed by Papp and Chen (1994).

4.1 Two-phase flow and measurement apparatus

The test bench used in the present study comprises a normal triangular tube bundle subjected to two-phase air - water vertical upward crossflow. Regarding the apparatus devoted for two-phase flow generation, the experimental facility consists of injection and conditioning sections, a water loop and air compression and conditioning systems. The water loop comprises a reservoir, a 15 CV centrifugal pump, electromagnetic volumetric flow transducers, a heat exchanger to control water temperature, and a perforated tube injector. Air is compressed by a 40 HP rotary screw compressor, and passes sequentially by a heat exchanger, reservoir, regulating pressure valve, turbine volumetric flow meters, needle and globe valves and is injected by 7 membrane injectors. The water is injected in the bottom region of the test section, and then is mixed with air just downstream. The two-phase mixture passes by a static mixer just upstream the test section. The static mixer is installed to obtain uniform phases distribution along the inlet cross section, with the objective of mimicking the flow inside a large scale heat exchanger; consequently, the flow pattern is defined by the tube bundle geometry and operational conditions as long as the inlet conditions are minimally uniform. Design and instrumentation of the experimental facility are detailed in Kanizawa and Ribatski (2016b).

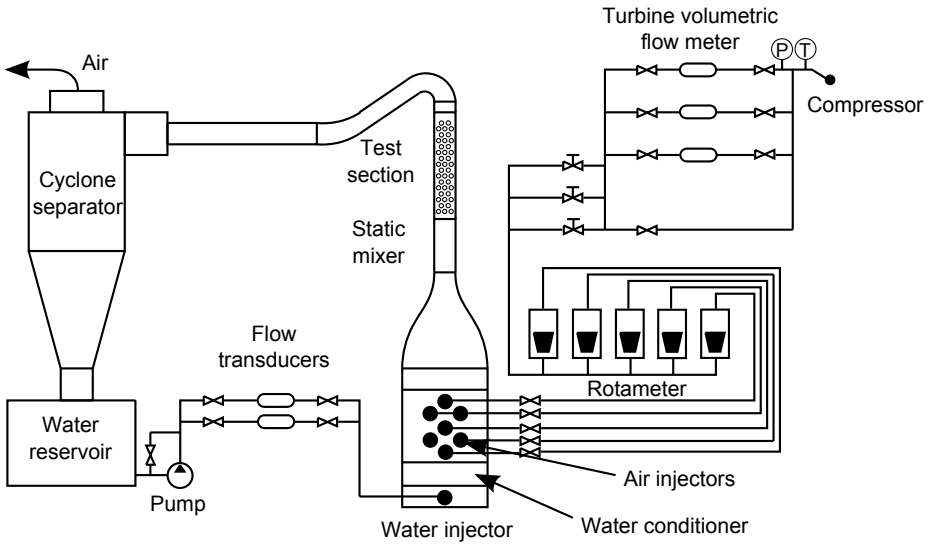

Figure 1. Scheme for the experimental facility used in the present study.

The test section consists of a triangular tube bundle, counting with 19 mm (3/4") O.D., 2 mm wall thickness, 381 mm long stainless steel tubes, with transverse pitch-to-diameter ($\tau = P/d$) ratio equal to 1.26. The tubes are distributed in 20 rows, where even rows have 4 tubes and odd rows have 3 tubes plus two half tubes positioned on the lateral walls to avoid bypass flow. Thus, the experiments are performed for upward crossflow condition. Downstream the test section, the flow is directed to a cyclone type separator, from which the water is directed to the reservoir and the air to laboratory outside.

Regarding to the tube bundle mounting, all tubes are rigidly installed, except the instrumented tube which is 378 mm long. This tube is cantilevered mounted on an end plate of the test section and it is located at the center of the 13th row. For the sake of experimental conditions repeatability, the tube has been installed at a zone where the two-phase flow is considered developed. Even though the flow characteristics continually change along the flow path due to variation of gas specific volume, the flow can be considered developed after the stabilization of flow pattern and negligible variation of flow parameters, such as pressure drop gradient. The required length, or number of rows in the case of external flow across tube bundles, for flow development depends on the inlet and operational conditions, as well as on the channel geometry. Hence, the tube bundle itself determines the phases distribution and mixing. In this context, Kanizawa and Ribatski (2016a) addressed criteria to characterize flow development during two-phase upward crossflow in tube bundles, which is based on the pressure gradient measurements; and for the present tube bundle geometry, the flow can be considered developed downstream the seventh tube row. Therefore, the instrumented tube is installed downstream the number of rows required for flow development. Moreover, this criterion is supported by the findings of Kondo and Nakajima (1980). They found that, under conditions of two-phase flow, reduced flow velocities and for transverse pitch-to-diameter of 1.28, the flow is completely developed after the eleventh tube row. The authors also indicated that the number of tube rows required for the flow development increases with increasing the transverse pitch-to-diameter ratio. Nonetheless, Kondo

and Nakajima (1980) performed experiments for very low flow velocities, characteristic of kettle reboilers.

The dynamic response of the cantilevered tube is measured by piezoelectric uniaxial microaccelerometers model 352A24, from PCB Piezotronics. They are installed inside the tube, with the sensing axes perpendicular to each other, and aligned with transverse and drag acceleration components. This set-up is presented in Fig.2. Data is acquired with a LMS SCADAS Mobile system running LMS Test.Lab. The present authors have devised the methodology for data acquisition and signal processing based on both, the form that these results are typically presented in the recent literature as well as on the qualitative evolution of the data during the initial runs. Based on these criteria, the acceleration was measured in periods of 8 s, with a sampling frequency of 2048 Hz and a resolution of 0.125 Hz. The analyzed PSDs are the result of 40 linear averages.

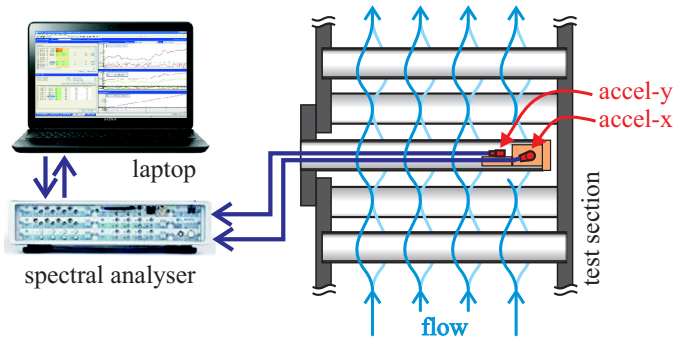

Figure 2. Set-up scheme for measuring tube response.

4.2 Reproducible experimental conditions

The flow conditions set in the present study were previously defined with the homogeneous void fraction model because of its ease of implementation. In this manner, distinct gas and liquid superficial velocities combinations were tested at void fractions (α) varying from 30 to 95%. These experimental conditions were represented in the flow pattern map proposed by Kanizawa and Ribatski (2016a), which is shown in Fig. 3. This flow pattern map was developed based on experimental database obtained in the present test section, and according to subjective and objective methods (Kanizawa and Ribatski, 2016a).

As it can be seen in Fig. 3, and based on the analysis presented by Kanizawa and Ribatski (2016a), the following flow patterns were identified for air-water upward crossflow in tube bundle: bubbles, churn, intermittent and annular. However, in the current study, only bubbles, churn and intermittent flow patterns are covered due to the experimental range.

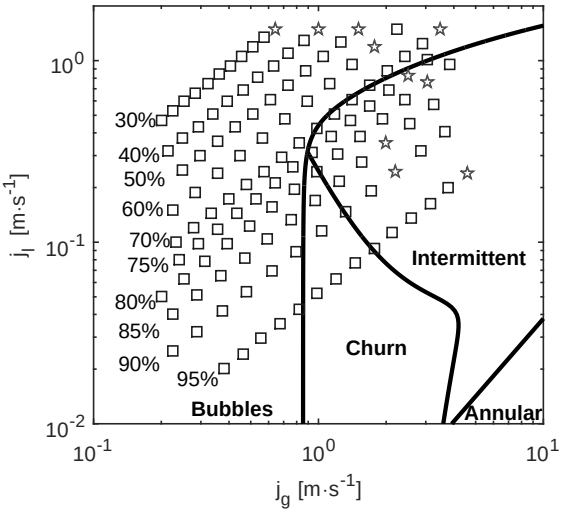

Figure 3. Flow pattern map for air-water flows ($p = 95kPa$; $T = 25°C$) according to Kanizawa and Ribatski (2016a). Pentagram markers correspond to half the mass flux for fluidelastic instability threshold according to Connors' model.

5. RESULTS

The results obtained in the present experimental study are organized in two sections. First, original results of hydrodynamic mass and two-phase damping ratio are presented. Subsequently, three distinct design guidelines to estimate turbulence-induced vibration are validated.

Hydrodynamic mass

In order to calculate hydrodynamic mass with Eq. 1, the first resonance frequency of the instrumented tube was identified from acceleration PSDs measured for each experimental condition. In this case, the resonance frequencies are picked from PSDs measured at mass velocities roughly half the velocity for fluidelastic instability (FEI). This constraint in mass velocity was imposed since Pettigrew *et al.* (1989) noted that the tube resonance frequency must be measured at mass fluxes sufficiently below FEI threshold, otherwise significant shifts in its value can be observed. In this way, the Connors' criterion for FEI was used as reference, $U_c/fd = K(2\pi\zeta m/\bar{\rho}d^2)^{0.5}$, where U_c/fd is the dimensionless flow velocity for FEI threshold, $(2\pi\zeta m/\rho d^2)$ is the mass-damping parameter and K is the fluidelastic constant. In this case, as suggested in Blevins (2001) for triangular tube bundles K is set to 2.8. The results are depicted in Fig.4.

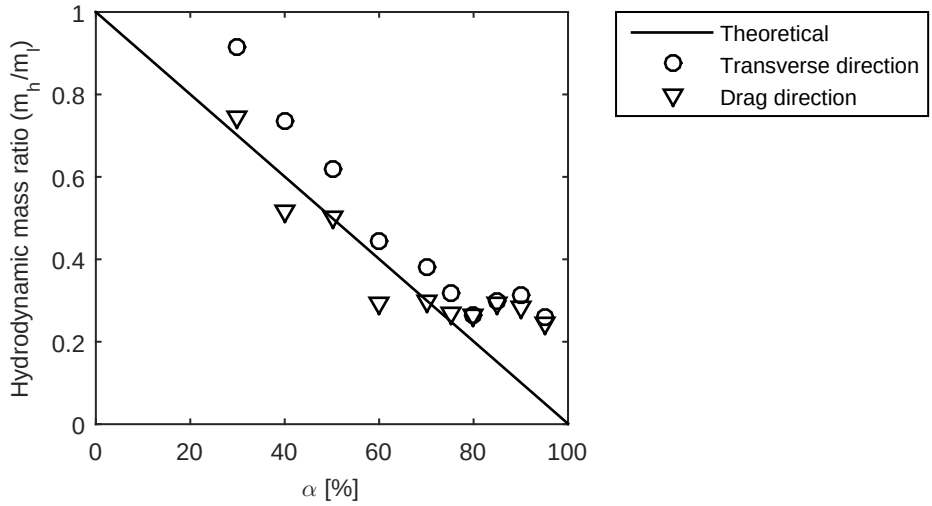

Figure 4. Hydrodynamic mass as a function of void fraction for mass velocities at roughly half the velocity for FEI: $G_{30} = 1498$; $G_{40} = 1498.4$; $G_{50} = 1498.9$; $G_{60} = 1191.3$; $G_{70} = 1501.1$; $G_{75} = 835.9$; $G_{80} = 761.7$; $G_{85} = 353.5$; $G_{90} = 246.7$; $G_{95} = 246.2\ kg/m^2s$.

According to Fig.4, the experimental results for hydrodynamic mass show a reasonable agreement with those predicted by Rogers *et al.* (1984) through Eq. 2, that is, hydrodynamic mass decreases linearly with void fraction increment. Even though hydrodynamic mass ratios accomplish the expected tendency, it can be noticed that hydrodynamic mass ratios in transverse direction are higher than those measured in drag direction for void fractions up to 75%. This difference between drag and transverse directions must be related to the distinct orientation and distance of neighboring tubes; while in the transverse direction there is one tube immediately adjacent at both sides, in drag direction there is a gap between adjacent tubes in the upper and lower rows. In this sense, it is important to notice that Eq. 2 does consider the confinement effect, but it does not differentiate between transverse and drag direction.

For $\alpha > 80\%$, hydrodynamic mass ratio values in transverse and drag directions are more similar if compared with results obtained for lower void fractions. However, it can be seen that hydrodynamic mass values present noticeable differences if compared with the theoretical model. This difference was also reported in Pettigrew *et al.* (1989) and may be attributed to the fact that these experimental conditions correspond to intermittent flow pattern, which in fact presents distinct phases velocities. Thus, the homogeneous model hypothesis of equal superficial velocities fails to model the actual flow kinematics. Actually, a higher slip between the phases is expected under these conditions, which would lead to higher liquid hold up and consequently to a higher added mass.

In general, according to the open literature (Carlucci and Brown, 1983; Pettigrew *et al.*, 1989, 1995, 2002), as well as with the present experimental results, the hydrodynamic mass ratio during cross flow agrees with the model proposed in Rogers *et al.* (1984) expanded for two-phase flow.

Two-phase damping ratio

Regarding to two-phase damping ratio measurements, the random vibration method is used to estimate total damping ratio values during two-phase crossflow. For this purpose, it was considered that two-phase flow delivers a random dynamic force to the tube as a white noise. Thus, the measured PSD will appear similar to a frequency response function (FRF), and PSD amplitudes at resonance frequency (f) and half-power frequencies (f_1 and f_2) will have the same ratio as in a FRF. In this manner, the half-power bandwidth formulation can be used to calculate the total damping ratio, which is given by (Maia and Silva, 1998)

$$\zeta_T = \frac{f_2 - f_1}{2f} \tag{15}$$

Structural damping can be obtained experimentally; in fact, previously performed dynamic tests showed that structural damping ratio is equal to 4.89% for transverse direction and 4.67% for drag direction. Moreover, viscous damping ratio can be calculated with Eq. 5. These values are subtracted from ζ_T to obtain ζ_{TP} in both transverse and drag direction.

The influence of mass velocity on damping ratio (excluding the structural component since is constant for all the conditions) was checked in the present study, and the experimental results are presented in Fig.5. Mass velocities up to half those necessary for fluidelastic instability were used. As it can be noticed from Fig.5, damping ratios in transverse and drag directions present distinct behaviors with mass velocity. For lower mass velocities ($G \leq 500 kg/m^2 s$), although data do not present a defined tendency, it can be seen that damping measurements in transverse direction are roughly higher than those in drag direction. Actually, in this mass velocity range, it can be noticed that the measured damping ratios are higher in transverse direction at $\alpha = 50\%$. For mass velocities higher than 500 $kg/m^2 s$, it can be seen that damping ratio in drag direction presents a defined increasing tendency with increasing mass velocity, which is more noticeably for $\alpha = 30\%$, 50% and 75%. In counterpart, damping ratios measured in transverse direction at high mass velocities present an irregular behavior; their values at $\alpha = 30\%$ and 50% vary more than 100%, and its value at $\alpha = 75\%$ decreases and subsequently stabilizes. As it can be noticed, it is difficult to draw a general conclusion about damping ratio dependence on mass velocity. However, at least for results in drag direction at $\alpha = 30\%$, 50% and 75%, it can be seen that damping increases with increasing mass velocity.

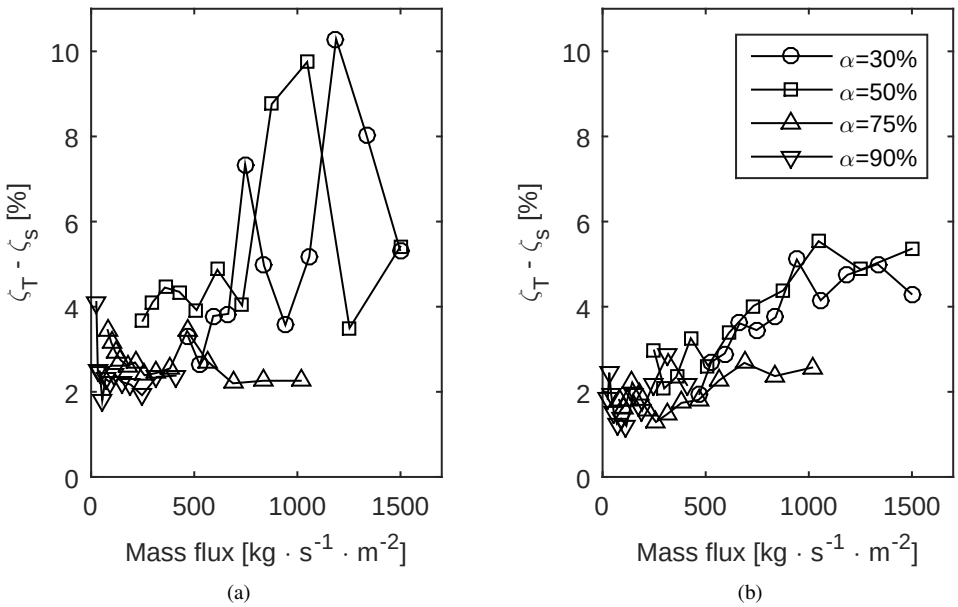

Figure 5. Effect of mass flux on tube damping in two-phase crossflow, (a) transverse direction and (b) drag direction.

The influence of void fraction on damping has also been checked in the present study. With the aim of simplifying the analysis and making it comparable with results presented in the literature, the experiments were performed for velocities equal to half of the fluidelastic instability threshold, similar to the conditions adopted for determination of hydrodynamic mass. Moreover, as generally practiced in open literature, the analysis of damping results is proposed in terms of the homogeneous void fraction. The obtained experimental results are depicted in Fig. 6, and, according to this figure, two-phase damping ratio does vary significantly with void fraction. Moreover, the results depicted in Fig. 6 show higher damping ratios in the transverse direction at intermediate void fractions with a maximum at α =40% and, with subsequent increment of void fraction, the damping ratio decreases until the condition of gas single-phase flow. Conversely, the

damping ratio in drag direction does not present that strong tendency registered in transverse direction. In drag direction, the maximum damping ratio was registered for α =50%, however, the damping ratio at α =40% is lower than that measured at α =30% and similar to that measured at α =60% and 70%. If values of damping ratio in both directions are compared, one can say that they are very similar, except for the values at α =40%, where damping ratio in transverse direction is 91% greater than in drag direction. Thus, excluding the results at α =40%, the average damping ratio is a representative indicator of damping in both directions. Even though experimental conditions for α <30% were unable to be set, one can notice that the two-phase damping ratio for α =0% is negligible if compared to that registered at intermediate void fractions. This behavior seems to agree, at least for the investigated void fractions, with the tendency of the data reported in the open literature (Carlucci and Brown, 1983; Pettigrew *et al.*, 1989; Lian *et al.*, 1997; Pettigrew *et al.*, 2001), which mention a peaking behavior of damping ratio with void fraction, with maximum damping at intermediate void fractions.

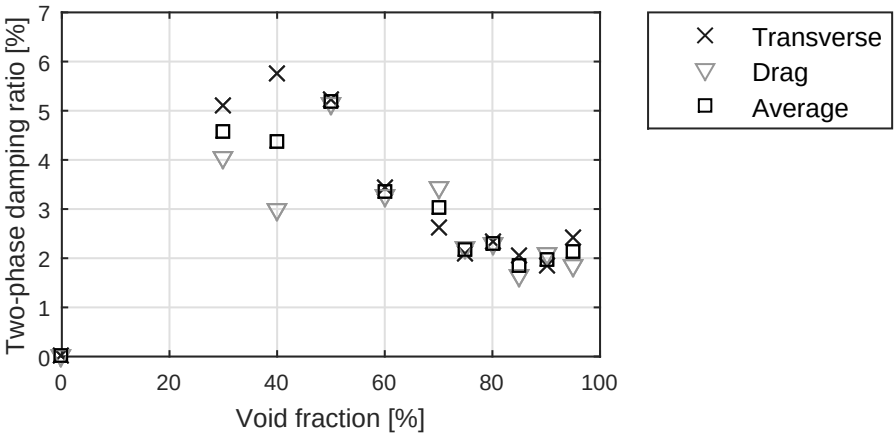

Figure 6. Two-phase damping ratio measurements.

These results also can be discussed in terms of flow patterns by using the map provided in Fig. 3. Damping measurements up to $\alpha = 70\%$ correspond to bubbles flow pattern. Moreover, the maximum damping value was measured under dispersed bubbles flow pattern, which is a particular condition of bubbles pattern with high liquid velocity and intermediate gas velocity. Intermittent flow pattern was registered from $\alpha = 75\%$ to 95%; lower two-phase damping ratios were measured in this void fraction interval. This contrasts with the result reported by Lian *et al.* (1997) that found higher damping during intermittent flow pattern, however, it must be pointed out that he used a flow pattern map proposed by Pettigrew *et al.* (1989) that present distinct transition lines distribution.

In order to compare the obtained results with a compilation of experimental data measured in distinct normal triangular tube bundles during air-water two-phase flow, the data must be normalized by the mass ratio and confinement factor. Such results can be found in Fig. 7. As it can be noticed, ζ_{TPn} becomes larger especially at low void fractions. Actually, normalized two-phase damping at $\alpha = 30\%$ is even larger than that at $\alpha = 50\%$, which is due to the large hydrodynamic mass measured at that void fraction. Despite of this, normalized two-phase damping until $\alpha = 50\%$ is noticeably higher than those at high void fraction, which confirms the behavior discussed previously. Furthermore, ζ_{TPn} measured at $\alpha \geq 60\%$ agrees with the available data for two-phase air - water upward cross flow in normal triangular tube bundles.

The results and the design guideline proposed by Pettigrew and Taylor (2004) are compared in Fig. 7. As it can be seen, the semi-empirical model proposed by Pettigrew and Taylor (2004) successfully predicts the minimum values for the examined void fractions. An exception can be opened at $\alpha = 75\%$, which is slightly under the estimated value. As a conclusion, it can be suggested that care must be exercised when selecting the value of A at design stage to avoid the possibility of estimating a larger damping than actual.

Turbulence-induced vibration design guidelines

Figure 8 depicts the comparison between $NPSD$ experimental results and the design guideline proposed by Taylor *et al.* (1989). As it can be seen, this design guideline accomplishes its goal, that is to calculate an upper-bound on $NPSD$ values within $25\% < \alpha < 90\%$. Also, it was verified that for $\alpha \geq 80\%$ the slope of experimental results increases. Actually, at $\alpha = 95\%$ the result are slightly higher than those predicted by Eq.10, which is beyond the validity range of the method proposed in Taylor *et al.* (1989).

The coefficient of interaction, as proposed in Papp and Chen (1994), was calculated according to Eq. 11 for all the experimental conditions tested in the present work. The results for transverse and drag directions are depicted in Fig.9 against the homogeneous void fraction. In addition, the standard deviation of C_I data normalized by its mean value,

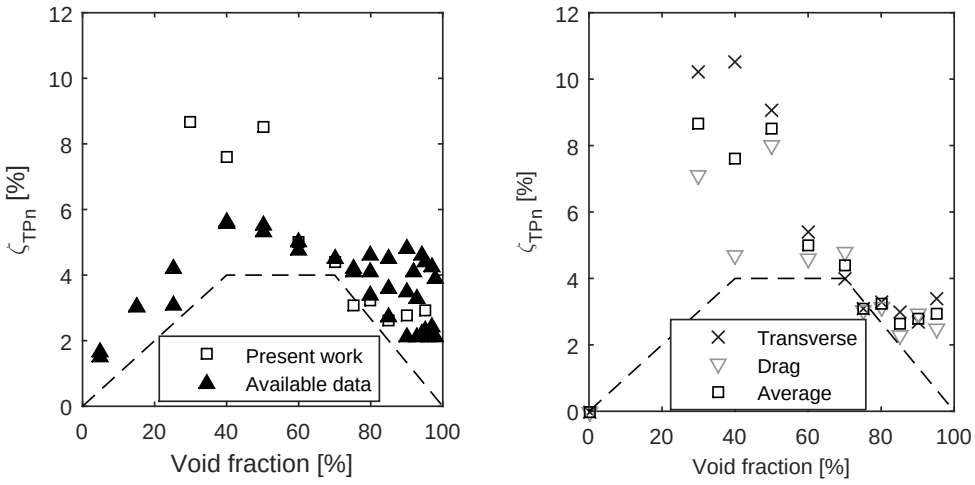

Figure 7. (a) Comparison between the design guideline and available damping data collected (Pettigrew and Taylor, 2004) with normalized damping ratio obtained in the present work, (b) Comparison between the design guideline and the results found in the present work. Dashed line is the design guideline proposed by Pettigrew and Taylor (2004).

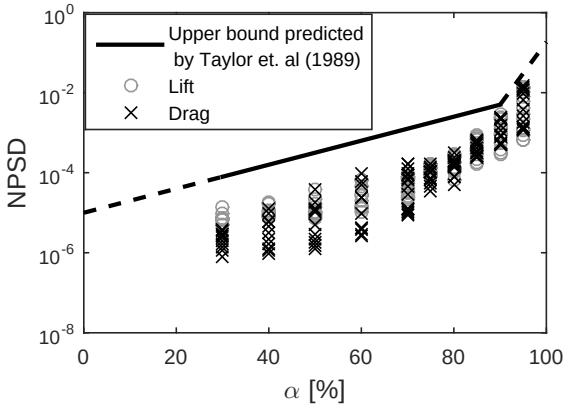

Figure 8. Normalized power spectral density of random turbulence excitation (NPSD) for normal triangular tube bundle, $\tau = 1.26$, $f = 105.24$Hz.

σ/C_I, was calculated and shown in Fig.9.

As it can be seen from Fig. 9, the values of C_I in both directions are in the same order for void fractions up to 60%, however, from a strict point of view, the values obtained in the present study are one order of magnitude lower if compared with those proposed in Papp and Chen (1994). Some factors can be pointed out as decisive in these results, perhaps the most remarkable difference is that the tube response data used in Papp and Chen (1994) is two orders of magnitude higher than the response measured in the present work considering the same mass velocity range. Furthermore, the standard deviation of C_I data (σ/C_I) is also analyzed for each void fraction. As it can be seen in Fig. 9, the standard deviation for $\alpha \leq 60\%$ in the transverse direction is lower than 24.35% of C_I mean value, and for drag direction it is limited to 35.13%. Assuming that C_I presents a normal distribution, these results show that, for $\alpha \leq 60\%$, there is a probability of 68% that the actual C_I value is at least 24.35% and 35.13% higher than the C_I mean value in transverse and drag directions, respectively. This result suggests that the adoption of maximum C_I as design criteria is more appropriate for $\alpha \leq 60\%$ than the C_I mean value.

On the other hand, the design guideline proposed by de Langre and Villard (1998) was also implemented for the present results. The upper-bound for the dimensionless reference equivalent force spectrum, $\left[\bar{\Phi}_E^0\right]_U$, is plotted in Fig. 10 and compared with the experimental results. As it can be seen, the design guideline proposed by de Langre and Villard (1998) effectively define an upper-bound for turbulence-induced vibration mechanism.

6. CONCLUSIONS

Based on the results obtained in the present work, the following conclusions can be drawn:

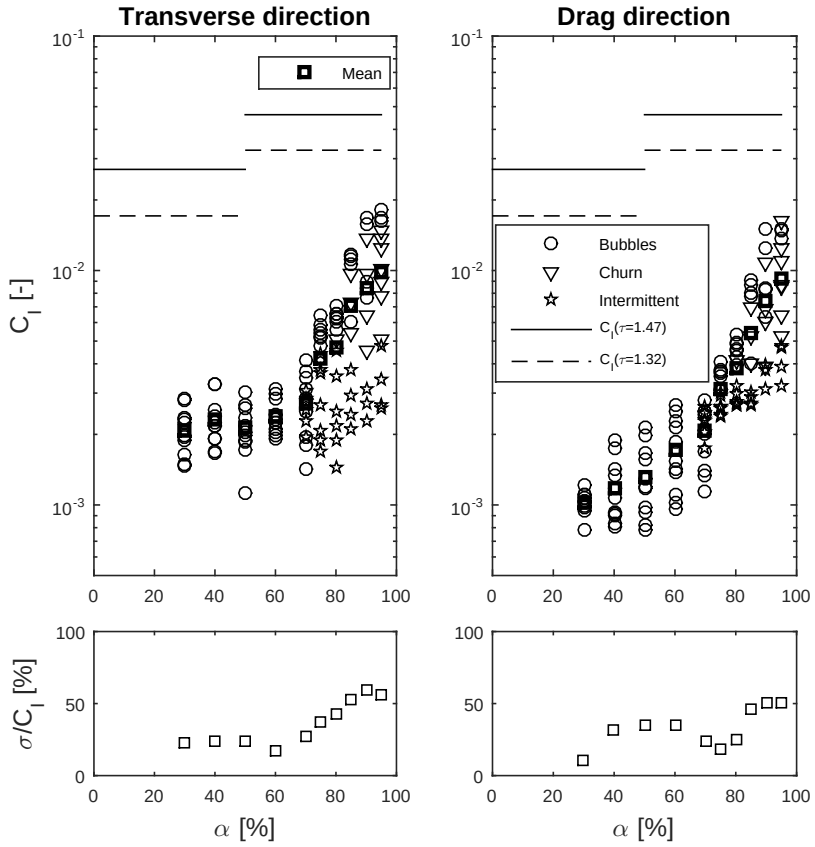

Figure 9. Coefficient of interaction for normal triangular tube bundle, $\tau = 1.26$, $f = 105.24$Hz, and C_I values proposed by Papp and Chen (1994) for normal triangular tube bundles with $\tau = 1.47$ e 1.32.

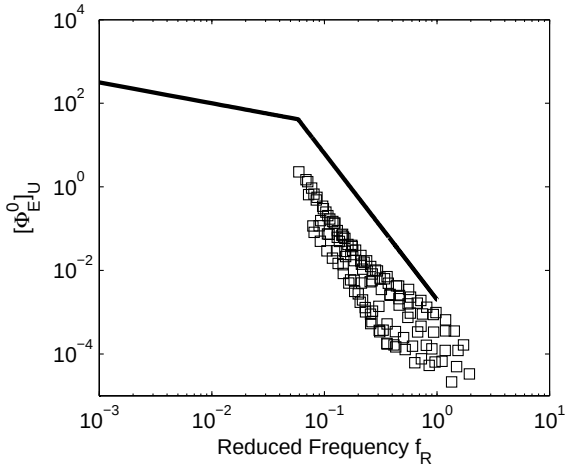

Figure 10. Upper-bound proposed in de Langre and Villard (1998) and experimental results obtained in the present work.

- Hydrodynamic mass and two-phase damping ratio measured in the present test section do depend on void fraction. Experimental results on hydrodynamic mass are relatively well represented by the available analytical model. In the case of two-phase damping ratio, the obtained results agree with the current semi-empirical guideline found in literature.
- Three distinct design guidelines, aiming to estimate the vibration severity in a tube bundle, were implemented for the experimental conditions performed in the present study. It was found that the upper bound for the normalized force spectra ($NPSD$) and for the dimensionless reference equivalent force spectrum, $\left[\bar{\Phi}^{0}_{E}\right]_{U}$, effectively define a maximum limit for the forces that would be occurring in the tube bundle. Conversely, the values of the coefficient

of interaction found for the present experimental study disagree with those proposed by Papp and Chen (1994). Although the present values of C_I are distinct, this guideline can be used as the basis for future studies in which other correlations are used for estimate the effects considered in the model, preferring those that better represent the phenomena taking place in the test section.

7. ACKNOWLEDGEMENTS

The authors acknowledge the financial assistance of the Brazilian National Council for Scientific and Technological Development - CNPq (grant numbers 481044/2010-8 and 307369/2013-7) and the doctorate scholarships awarded to the first and second authors by CAPES Foundation and the São Paulo Research Foundation - FAPESP (grant numbers 2010/20670-2 and 2014/06902-9), respectively.

8. REFERENCES

Álvarez-Briceño, R.P., Kanizawa, F.T., Ribatski, G. and de Oliveira, L.P.R., 2016. "Validation of turbulence induced vibration design guidelines in a normal triangular tube bundle during two-phase crossflow". *Journal of Fluids and Structures*, p. Under Review.

Axisa, F., Antunes, J. and Villard, B., 1990. "Random excitation of heat exchanger tubes by cross-flows". *Journal of Fluids and Structures*, Vol. 4, pp. 321–341.

Blevins, R.D., 2001. *Flow-Induced Vibration*. Krieger Publishing Company, Malabar, Florida, 2nd edition.

Carlucci, L.N., 1980. "Damping and hydrodynamic mass of a cylinder in simulated two-phase flow". *ASME Journal of Mechanical Design*, Vol. 102, pp. 597–602.

Carlucci, L.N. and Brown, J.D., 1983. "Experimental studies of damping and hydrodynamic mass of a cylinder in confined two-phase flow". *Journal of Vibration, Acoustics, Stress, and Reliability in Design*, Vol. 105, No. 1, pp. 83–89.

Collier, J. and Thome, J.R., 1994. *Convective Boiling and Condensation*. Oxford Science Publications, Oxford, 3rd edition.

de Langre, E. and Villard, B., 1998. "An upper bound on random buffeting forces caused by two-phase flows across tubes". *Journal of Fluids and Structures*, Vol. 12, pp. 1005–1023.

Grant, I.D.R. and Chisholm, D., 1979. "Two-phase flow on the shell-side of a segmentally baffled shell-and-tube heat exchanger". *Journal of Heat Transfer*, Vol. 101(1), pp. 38–42.

Green, S.J. and Hetsroni, G., 1995. "Pwr steam generators". *International Journal of Multiphase Flow*, Vol. 21, pp. 1–97.

Kanizawa, F.T. and Ribatski, G., 2015. "Void fraction predictive method based on the minimum kinetic energy". *Journal of the Brazilian Society of Mechanical Sciences and Engineering*, Vol. 38, pp. 209–225.

Kanizawa, F.T. and Ribatski, G., 2016a. "Two-phase flow patterns across triangular tube bundles for air-water upward flow". *International Journal of Multiphase Flow*, Vol. 80, pp. 43–56.

Kanizawa, F.T. and Ribatski, G., 2016b. "Void fraction and pressure drop during external upward two-phase crossflow in tube bundles - part i: Experimental investigation". *International Journal of Heat and Fluid Flow*, Vol. In Press.

Kanizawa, F.T. and Ribatski, G., 2016c. "Void fraction and pressure drop during external upward two-phase crossflow in tube bundles - part ii: Predictive methods". *International Journal of Heat and Fluid Flow*, Vol. In Press.

Khushnood, S., Khan, Z.M., Malik, M.A., Koreshi, Z., Javaid, M.A., Khan, M.A., Qureshi, A.H., Nizam, L.A., Bashir, K.S. and Hussain, S.Z., 2012. *Cross-Flow-Induced-Vibrations in Heat Exchanger Tube Bundles: A Review, Nuclear Power Plants*. InTech, Riteja, 1st edition.

Kondo, M. and Nakajima, K.I., 1980. "Experimental investigation of air-water two phase upflow across horizontal tube bundles: Part 1, flow pattern and void fraction". *Bulletin of JSME*, Vol. 23(117), pp. 385–393.

Lian, H.Y., Noghrehkar, G., Chan, A.M.C. and Kawaji, M., 1997. "Effect of void fraction on vibrational behavior of tubes in tube bundle under two-phase cross flow". *Journal of vibration and acoustics*, Vol. 119, No. 3, pp. 457–463.

Maia, N. and Silva, J., 1998. *Theoretical and Experimental Modal Analysis*. Research Studies Press LTD, Hertfordshire, 1st edition.

Noghrehkar, G., Kawaji, M. and Chan, A., 1999. "Investigation of two-phase flow regimes in tube bundles under cross-flow conditions". *International Journal of Multiphase Flow*, Vol. 25, pp. 857–874.

Païdoussis, M.P., Price, S.J. and de Langre, E., 2011. *Fluid-structure interactions: cross-flow-induced instabilities*. Cambridge University Press, 1st edition.

Papp, L. and Chen, S.S., 1994. "Turbulence-induced vibration of tube arrays in two-phase flow". *Journal of Pressure Vessel Technology*, Vol. 116, pp. 312–316.

Pettigrew, M.J., Rogers, R.J. and Axisa, F., 1986. "Damping of multispan heat exchangers tubes - part2: In liquids". In *ASME Pressure Vessels Symposium on Special Topics of Structural Vibration, and Piping Conference*. Chicago, USA, pp. 89–98.

Pettigrew, M.J., Taylor, C. and Kim, B., 1989. "Vibration of tube bundles in two-phase cross-flow: Part 1 - hydrodynamic mass and damping". *Journal of Pressure Vessel Technology*, Vol. 111, pp. 466–477.

Pettigrew, M.J. and Taylor, C.E., 1994. "Two-phase flow induced vibration: An overview". *Journal of Pressure Vessel Technology*, Vol. 116, pp. 233–253.

Pettigrew, M.J. and Taylor, C.E., 2003. "Vibration analysis of shell and tube heat exchangers: an overview - part 2. vibration response, fretting-wear, guidelines". *Journal of Fluids and Structures*, Vol. 18, pp. 485–500.

Pettigrew, M.J. and Taylor, C.E., 2004. "Damping of heat exchanger tubes in two-phase flow: Review and design guidelines". *Journal of Pressure Vessel Technology*, Vol. 126, pp. 523–533.

Pettigrew, M.J., Taylor, C.E., Janzen, V.P. and Whan, T., 2002. "Vibration behavior of rotated triangular tube bundles in two-phase cross flows". *Journal of Pressure Vessel Technology*, Vol. 124, pp. 144–153.

Pettigrew, M.J., Taylor, C.E., Jong, J.H. and Curie, I.G., 1995. "Vibration of a tube bundle in two-phase freon cross flow". *Journal of Pressure Vessel Technology*, Vol. 117, pp. 321–329.

Pettigrew, M.J., Taylor, C.E. and Kim, B.S., 2001. "The effects of bundle geometry on heat exchanger tube vibration in two-phase cross flow". *Journal of Pressure Vessel Technology*, Vol. 123, pp. 414–420.

Rogers, R.G., Taylor, C. and Pettigrew, M.J., 1984. "Fluid effects on multi span heat exchanger tube vibration". In *Proceedings of the ASME PVP Conference*. New York, EEUU, pp. 17–26.

Sim, W.G., 2007. "An approximate damping model for two-phase cross-flow in horizontal tube bundles". In *ASME Pressure Vessels and Piping Conference*. San Antonio, USA.

Taylor, C., Currie, I., Pettigrew, M.J. and Kim, B., 1989. "Vibration of tube bundles in two-phase cross-flow: Part 3 - turbulence-induced excitation". *Journal of Pressure Vessel Technology*, Vol. 111(4), pp. 488–500.

Zukauskas, A. and Ulinskas, R., 1983. *2.2.4 Banks of plain and finned tubes. In Heat Exchanger Design Handbook 2 - Fluid mechanics and heat transfer*. Hemisphere Publishing Corporation, United States of America, 1st edition.

9. RESPONSIBILITY NOTICE

The authors are the only responsible for the printed material included in this paper.